Check for updates

pH-Responsive Degradable Electro-Spun Nanofibers Crosslinked via Boronic Ester Chemistry for Smart Wound Dressings

Sofia Nieves Casillas-Popova, Nishadi Dilkushi Lokuge, Brandon Andrade-Gagnon, Farhan Rahman Chowdhury, Cameron D. Skinner, Brandon L. Findlay, and Jung Kwon Oh*

Recent advances in the treatment of chronic wounds have focused on the development of effective strategies for cutting-edge wound dressings based on nanostructured materials, particularly biocompatible poly(vinyl alcohol) (PVA)-based electro-spun (e-spun) nanofibers. However, PVA nanofibers need to be chemically crosslinked to ensure their dimensional stability in aqueous environment and their capability to encapsulate bioactive molecules. Herein, a robust approach for the fabrication of pH-degradable e-spun PVA nanofibers crosslinked with dynamic boronic ester (BE) linkages through a coupling reaction of PVA hydroxyl groups with the boronic acid groups of a phenyl diboronic acid crosslinker is reported. This comprehensive analysis reveals the importance of the mole ratio of boronic acid to hydroxyl group for the fabrication of well-defined BE-crosslinked fibrous mats with not only dimensional stability but also the ability to retain uniform fibrous form in aqueous solutions. These nanofibers degrade in both acidic and basic conditions that mimic wound environments, leading to controlled/enhanced release of encapsulated antimicrobial drug molecules. More importantly, drug-loaded BE-crosslinked fibers show excellent antimicrobial activities against both Gram-positive and Gram-negative bacteria, suggesting that this approach of exploring dynamic BE chemistry is amenable to the development of smart wound dressings with controlled/enhanced drug release.

S. N. Casillas-Popova, N. D. Lokuge, B. Andrade-Gagnon, C. D. Skinner, B. L. Findlay, J. K. Oh
Department of Chemistry and Biochemistry
Concordia University
Montreal, Quebec H4B 1R6, Canada
E-mail: john.oh@concordia.ca
F. R. Chowdhury, B. L. Findlay
Department of Biology
Concordia University
Montreal, Quebec H4B 1R6, Canada

1. Introduction

Chronic wounds, including large-area burns, full-thickness wounds, infected wounds, and diabetic wounds, are pathological conditions characterized by non-healing injuries requiring long recovery times.[1] They have become a major health concern in recent years because of their prevalence and rising incidence, which has seriously burdened the healthcare system.[2] Nowadays, the standard therapy relies on outdated practices such as nutritional support and infection control, which has proven to have limitations, particularly when a patient has co-morbidities,[3] and often leads to lower patient quality of life and life expectancy, increased health risks, elevated morbidity rates, and even patient mortality.[4] Hence, there is a significant need to develop effective therapies to replace the existing limited alternatives.

A better and potentially more effective approach to treat chronic wounds is to use wound dressings based on nanostructured materials that, in addition to their primary purpose as shielding materials, actively promote wound healing and prevent infections.[5] Electro-spun (e-spun) nanofibers based on poly(vinyl alcohol) (PVA) have been extensively explored as biocompatible nanostructured materials for wound dressings.[6] PVA possesses remarkable electrospinnability, thermal and chemical stability, high water-absorbing capacity, good biocompatibility and biodegradability, as well as FDA approval for biological uses. Because of its high water-solubility, PVA-based e-spun fibers need to be crosslinked in order to retain their dimensional stability in a biological (e.g., aqueous) environment. In contrast to physical crosslinking via heating[7] that frequently results in poor mechanical properties and short durability, covalent crosslinking has been extensively explored as an effective means to fabricate e-spun crosslinked PVA fibers.[8] Typically, isocyanate,[9] carboxylic acid,[10] and anhydride[11] crosslinkers have been used to crosslink PVA materials through the formation of carbamate or ester crosslinks with the pendant hydroxyl groups of PVA fibers. Since these crosslinks are permanent rather than labile in nature, these

**ADVANCED
SCIENCE NEWS**

www.advancedsciencenews.com
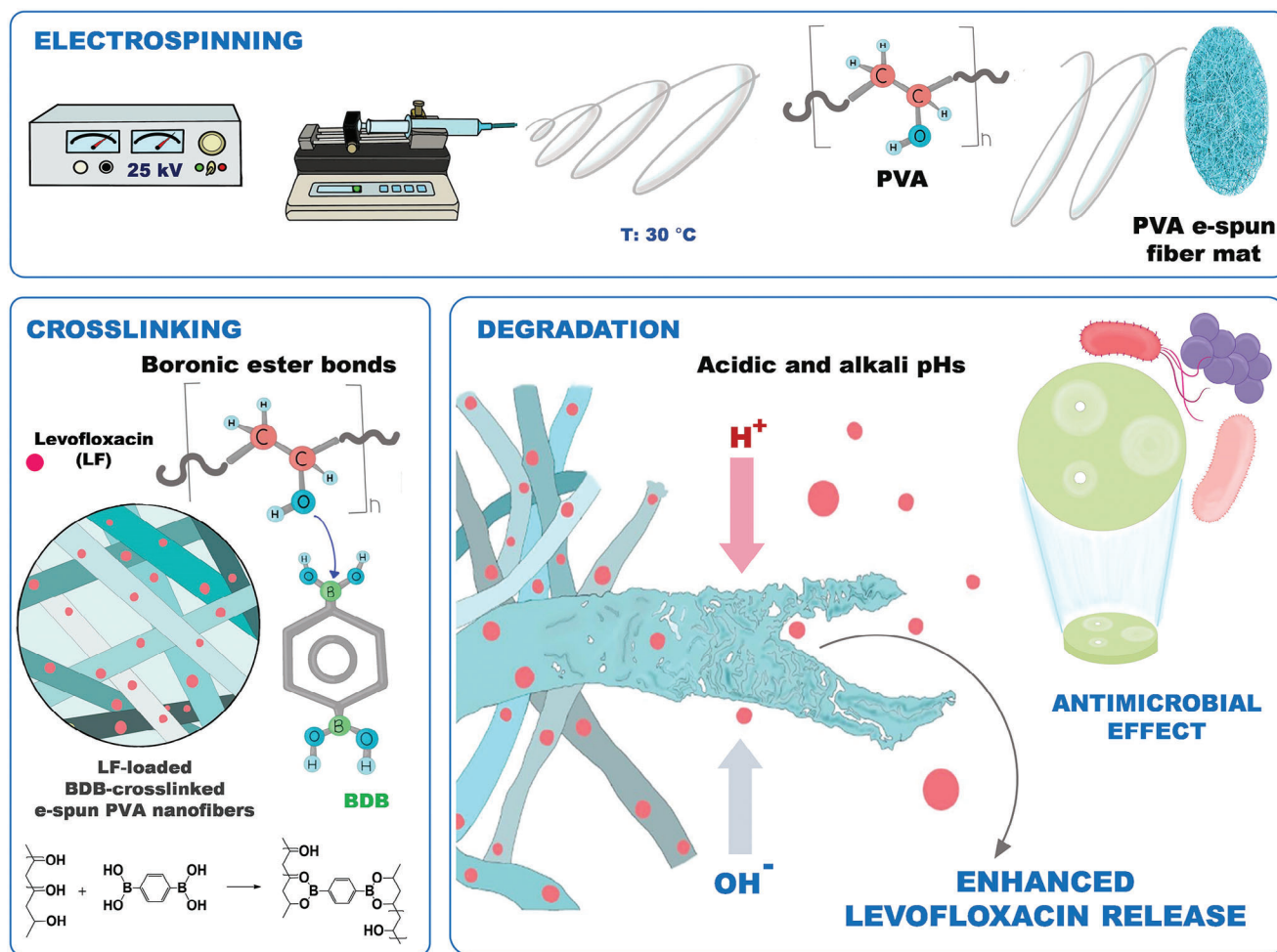
{M}acro-
molecular
Bioscience

www.mbs-journal.de

Figure 1. Schematic illustration of our proof-of-concept approach to crosslink PVA e-spun nanofibers via BE chemistry to fabricate pH-degradable BE-crosslinked e-spun PVA nanofibers for wound dressings exhibiting controlled/enhanced release of encapsulated drugs.

covalent crosslinking chemistries exhibit low degradability in the biological environment and uncontrolled release of encapsulated drug molecules in targeted wound sites. Further, those crosslinking reactions require harsh chemical processes and toxic catalysts that are incompatible with the body.[12]

Stimuli-responsive degradation (SRD) has been integrated into the fabrication of e-spun nanofibers of various polymeric materials mostly based on hydrophobic polymers.[13] These SRD-exhibiting nanofibers have been designed to degrade in response to external stimuli, typically pH change, thus to achieve slow, on-demand, or targeted release of encapsulated drugs.[14] Glutaraldehyde (GA) has been typically used to fabricate e-spun crosslinked PVA fibers through the formation of acid-labile acetal crosslinks.[15] However, there has been a growing concern over the cytotoxicity of unreacted GA residues left in the final products, which might eventually impair protein functioning and inhibit cellular processes.[16] Moreover, the formed alkylacetal crosslinks could exhibit slow cleavage through acid-catalyzed hydrolysis, similar to acetaldehyde acetal linkages in acidic pH at 4.0–5.0.[17]

Boronic ester (BE) bonds are labile and can be cleaved to the corresponding boronic acid and diol when exposed to reac-

tive oxygen species or pH change.[18] Diols can be as diverse as aliphatic diols or aromatic catechol derivatives, which broaden the applicability of degradable BE-based crosslinks to various polymeric materials. Owing to these features, BE bonds have been explored as biocompatible crosslinks for PVA materials, unfortunately, focusing mostly on three-dimentionally crosslinked hydrogels without considering other processing forms.[19] A few reports describe the feasibility of inorganic boric acid ($B(OH)_3$) to crosslink PVA e-spun nanofibers.[20] However, to our best knowledge, the use of organic diboronic acids, particularly phenyldiboronic acids, has not yet been explored as an effective means to fabricate BE-crosslinked e-spun PVA nanofibers exhibiting pH-responsive degradation and drug release, much less their potential application to smart wound dressings.

Herein, we report our proof-of-concept approach exploring pH-degradable BE chemistry in fabrication of effective pH-degradable BE-crosslinked e-spun PVA nanofibers (**Figure 1**). A phenyldiboronic acid was chosen as a model crosslinker as it can react with the pendant hydroxyl groups in PVA chains through esterification to form pH-cleavable BE crosslinks in e-spun nanofibrous mats. Our comprehensive characterization of BE-induced crosslinking, pH-responsive degradation,
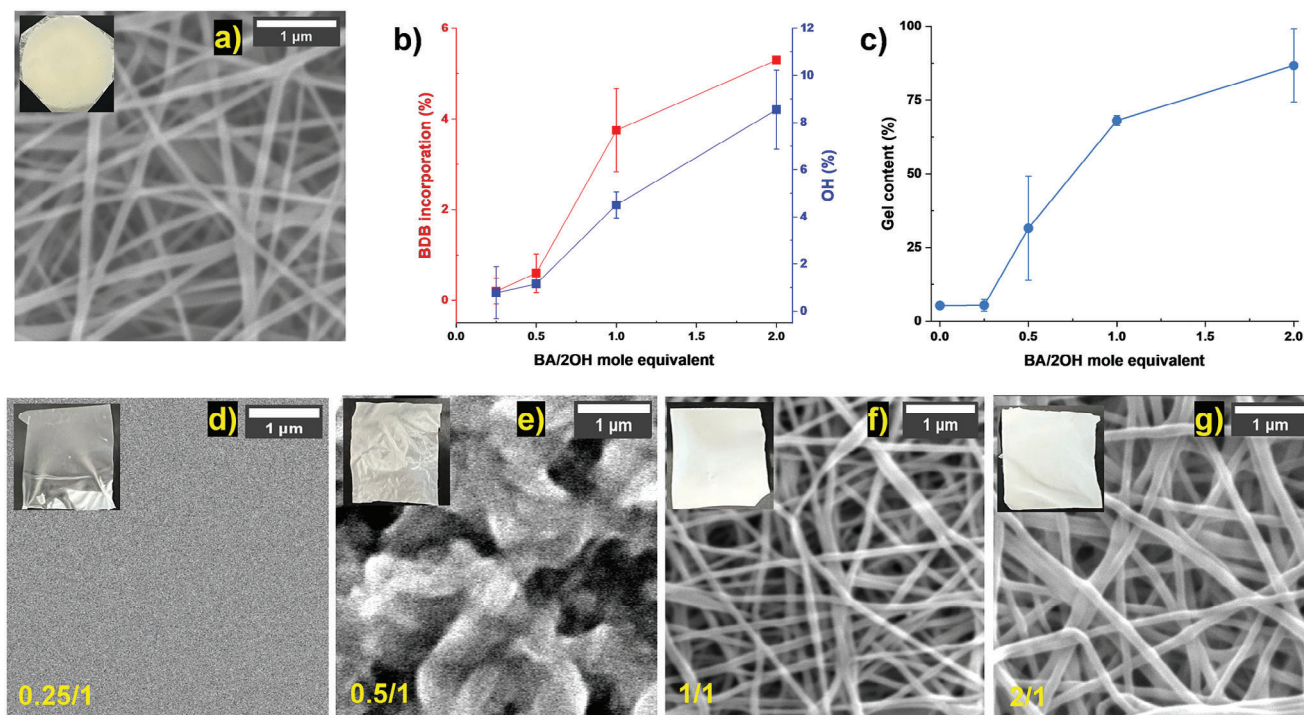
2400217 (2 of 9)

**ADVANCED
SCIENCE NEWS**

www.advancedsciencenews.com

[M] acro-
molecular

Bioscience

www.mbs-journal.de

Figure 2. a) SEM image of uncrosslinked PVA nanofibers; b) %BDB incorporated into PVA mats ($y1$-axis) and %OH groups reacted with BA in PVA mat, c) %insoluble PVA, and d) SEM images of BE-crosslinked PVA mats at various mole equivalent ratio of BA/2OH = 0.25, e) 0.5/1, f) 1/1, and g) 2/1. Insets in (d–g) are the digital images of mats after being immersed in water for 24 h and then dried. Scale bar for all SEM images = 1 µm.

encapsulation, and controlled drug molecule release confirms that this approach allows for the fabrication of novel dimensionally-stable BE-crosslinked PVA e-spun nanofibers degradable in acidic and alkali pHs. Furthermore, drug-loaded nanofibers possessed antimicrobial properties against both Gram-positive and Gram-negative bacteria (Figure 1).

2. Results and Discussion

Our experiments began with investigating the important parameters that significantly influence e-spinning and optimization of our lab-made instrument (see Figure S1, Supporting Information) with the goal of fabricating well-defined e-spun PVA nanofibers with uniform diameters across fibers and negligible presence of droplets or beads. Commercially-available PVA granules, with a molecular weight of 89–98 kg mol^{-1} as given by the supplier, were chosen to prepare a 10 wt% aqueous solution. The transparent, viscous PVA solution was e-spun with varying processing parameters including voltage (22, 25, or 27 kV), needle type (21G or 25G 1½), chamber temperature (23 or 30 °C), needle-collector distance (7, 9, or 14 cm), and feed rate (0.6–1.1 mL h^{-1}). The detailed experimental design, observations, and nanofibers produced are summarized in Table S1 (Supporting Information). Additionally, the undesired formation of micron-sized droplets, nanofibers with inconsistent diameters, or wavy nanofibers during e-spinning was illustrated in scanning electron microscopy (SEM) images (Figure S2, Supporting Information). Under the optimized conditions including 25 kV, 9 cm needle-collector distance, 25G 1½ needle, and 0.85 mL h^{-1} feed rate at 30 °C, well-defined e-spun PVA fibers were fabricated on aluminum substrates (digital images shown in the inset of **Figure 2a**). Their average diameters were determined to be 139.3 ± 34.7 nm, confirmed by SEM analysis (Figure 2a for images and Figure S3, Supporting Information, for diameter histogram).

The e-spun fibrous mats contained only PVA (not crosslinked) and were readily dissolved in water. To introduce crosslinking into the nanofibers with BE bonds, the PVA fiber mats were immersed in tetrahydrofuran (THF) containing a boronic acid crosslinker to induce the formation of BE linkages by the reaction of two hydroxyl groups in PVA and a boronic acid group in the crosslinker without aid of a catalyst at ambient temperature. 1,4-Benzenediboronic acid (BDB; functionality = 2) is commercially available and has been used as effective crosslinker for the fabrication of BE-crosslinked bulk hydrogels without aid of a catalyst at ambient temperature.[21,22] THF was chosen as it is a poor solvent for PVA and has a relatively low boiling point (66 °C) allowing for it to be removed from fibrous mats.

To gain insights into crosslinking PVA mats with BDB, the amount of BDB was varied as a mole equivalent ratio of boronic acid (BA)/2 hydroxyl (OH) group (BA/2OH) ranging from 0.25/1 to 2/1. Note that two OH groups react with one BA group to form one BE bond. The pieces of e-spun PVA mats (after the removal from the aluminum foil) were immersed in BDB-containing THF for 48 h and dried in a vacuum at 40 °C for 24 h to remove residual THF. All dried mats appeared to be opaque, suggesting that their nanofibrous structures were preserved during crosslinking in THF. To investigate the efficiency of crosslinking through the formation of BE bonds by the reaction of BA and OH groups, the amount of BDB incorporated into the mats was estimated by the weight difference of the PVA mats before and after

2400217 (3 of 9)

**ADVANCED
SCIENCE NEWS**

www.advancedsciencenews.com

[M]acro-
molecular
Bioscience

www.mbs-journal.de

treatment with BDB. Comparisons of the weight with the amount of BDB used in the recipe allowed the estimation of the %BDB incorporated. As seen in Figure 2b ($\gamma1$-axis), <0.4 mol% BDB was incorporated when the BA/2OH = 0.25/1 and 0.5/1. Upon increasing the mole equivalent of BA, the %BDB increased, but interestingly, it only reached a maximum of 5.3% even in the presence of large BA excess (BA/2OH = 2/1). Next, the amount of BDB incorporated into the fibrous mats was used to determine the mole% of the OH groups, in PVA, that had reacted with BDB to form the BE crosslinks (e.g., extent of crosslinking). As seen in Figure 2b ($\gamma2$-axis), it was calculated to be 0.1 mol% with BA/2OH to 0.25/1 and increased to 8.5 mol% at BA/2OH to 2/1. Our analysis suggests that the extent of crosslinking of PVA fibers appears to be limited to a maximum of 10 mol%.

Further, to confirm that the fabricated PVA mats were crosslinked, the dried mats after being treated with BDB were immersed in deionized water (pH = 6.2) for 24 h. As shown in the Supporting Information (Video clips S1 and S2), PVA mats treated with BDB (BA/2OH = 2/1) did not appear to dissolve in water, while uncrosslinked mats were quickly dissolved. Such comparison could suggest that BDB-treated PVA mats were essentially crosslinked and thus remained insoluble, rather swollen in an aqueous solution. The weight of the dried mats was measured before and after exposure to water to determine gel content. This method compared the weight of crosslinked nanofibers before and after being immersed in water as an indirect measure of the extent of crosslinking based on the amount of PVA insoluble in water. As seen in Figure 2c, the gel content was negligible with <5% for mats with no BDB and even 0.25/1 BA/2OH. Upon increasing BA/2OH, it increased and reached a maximum of 85% (15% loss of mass) with BA/2OH = 2/1, even though only 5.6% BDB was incorporated into the PVA mats. Given these results, SEM analysis was conducted to investigate the morphologies of crosslinked fibers (Figure 2d–g). PVA mats crosslinked with BA/2OH greater than 1/1 were opaque in their digital images and retained their fibrous forms in their SEM images (Figure 2e,f). Their average diameters were determined to be 137.6 ± 30.6 nm with BA/2OH = 1/1 and 133.9 ± 21.2 nm with BA/2OH = 2/1 (Figure S4, Supporting Information, for diameter histogram), which do not appear to be significantly changed upon crosslinking (139.3 ± 34.7 nm for uncrosslinked fibers). In contrast, mats crosslinked with a less amount of BDB as BA/2OH = 0.25/1 and 0.5/1 became transparent in their digital images and no fibrous forms were observed in their SEM images after being immersed in water (Figure 2d,e).

To confirm the formation of BE crosslinks, Fourier-transform infrared (FT-IR) spectroscopic analysis was conducted with PVA mats crosslinked with BA/2OH = 2/1. As compared in Figure S5 (Supporting Information), the FT-IR spectrum for BDB-crosslinked PVA mat exhibits two characteristic vibrational modes at 1302 and 660 cm^{-1} which correspond to B—O—C bending and O—B—O stretching frequencies, respectively.[21,23] These modes confirm the formation of BE bonds through the reaction of BA groups in BDB with OH groups in PVA, fabricating BDB-crosslinked PVA nanofibrous mats. Moreover, a large vibrational mode at 3320 cm^{-1} appeared in their FT-IR spectrum corresponds to the large excess of unreacted OH groups from the PVA, which is consistent with our analysis of %BDB and %OH groups in BDB-crosslinked mats.

Further, the BDB-crosslinked fibrous mats were characterized for their thermal properties using differential scanning calorimetry (DSC) analysis. As seen in Figure S6 (Supporting Information), the mats exhibit an increased glass transition temperature at 91.3 °C and a relatively broad melting transition at 207.6 °C, compared 80.8 and 224.1 °C for uncrosslinked mats respectively. Such increase in glass transition and decrease in melting transition is expected from successful crosslinking of PVA chains due to decreased mobility and packability of the PVA chains.

Overall, these results suggest that e-spun PVA fibers were crosslinked with BDB to form BDB-crosslinked PVA mats through the formation of BE crosslinks. To limit solubility of the fibers, in aqueous environments, a mole equivalent ratio of BA/2OH >1/1 is required.

In a separate experiment, methanol (MeOH) alone (with no BDB crosslinker) was tested for crosslinking e-spun PVA nanofibers since it has been used as a common solvent. Following a similar protocol, uncrosslinked e-spun PVA nanofibrous mats were immersed in MeOH, dried, and then immersed in water. As seen in Figure S7 (Supporting Information), the gel content (insoluble species in water) gradually increased and reached a plateau at 63% after immersion for 3 days in MeOH. This result means that PVA e-spun mats had 63% insoluble species (e.g., extent of crosslinking) in MeOH even without BDB crosslinker, which is quite different from that (<5%) when THF alone was used. The plausible reason is that MeOH induces physical crosslinking through hydrogen bonding in e-spun nanofibers as described in literature.[24]

Given the effect of the amount of BDB on crosslinking through the formation of BE crosslinks, BDB-crosslinked PVA mats fabricated with BA/2OH = 2/1 were investigated for their pH-responsive degradation. Pieces of the mats were incubated in aqueous buffer solutions across a broad range of pHs from 5 to 10.4. As seen in **Figure 3**a, gravimetry results determined the %degradation to be 12.4% at human pH (7.4) but increased in both acidic (25.7%) and alkali pHs (46.7%). The plausible reason for degradation loss at neutral pH could be ascribed to loosely intertwined polymer chains within the nanofibers. BE bonds are known to be sensitive to pH and were more extensively cleaved in both acidic and alkali conditions through mechanisms illustrated in Figure S8 (Supporting Information).[25] The digital images of the degraded mats incubated at the pHs appeared to be transparent (Figure 3b). Further analysis of their morphologies, as shown in SEM images of Figure 3c–f, reveals the loss of fibrous forms at all the pH ranges. An interesting observation was that the fibrous forms were slightly retained for mats incubated at pH = 7.4, compared with mats incubated at acidic and alkali pHs. These results illustrate increased %degradation at both acidic and alkali pHs, likely by hydrolysis of the BE bonds in PVA mats.

Despite the high solubility of PVA in water, the degraded crosslinked mats did not appear to fully dissolve in water. The most plausible reason is that during the crosslinking process intra- and inter-molecular hydrogen bonds between OH groups in the PVA chains are also created and are responsible for preventing the dissolution of PVA chains even after cleavage of the BE bonds.

We then investigated the feasibility of using BDB-crosslinked nanofibers exhibiting controlled release of drug molecules for wound dressings. Levofloxacin (LF), an antibiotic frequently
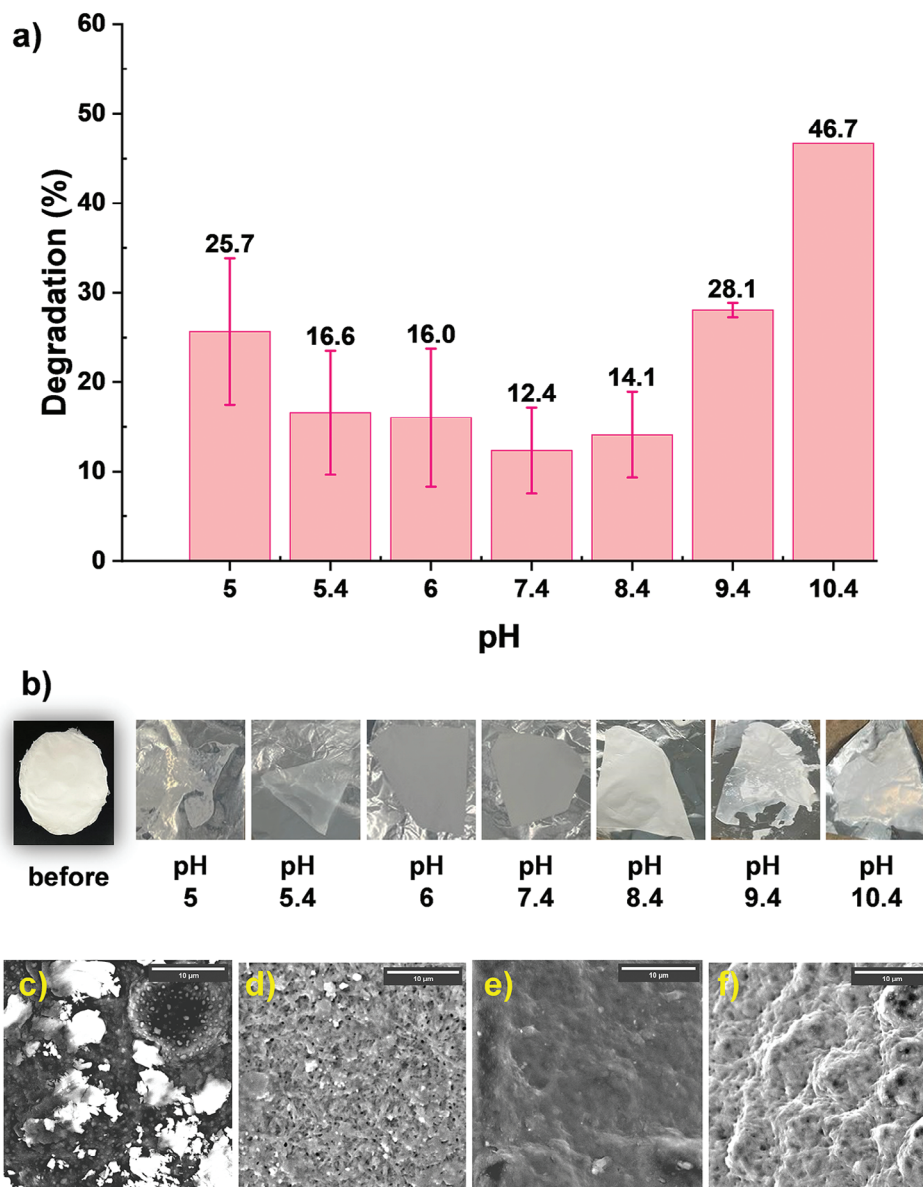
ADVANCED
SCIENCE NEWS

www.advancedsciencenews.com

Macro-
molecular
Bioscience

www.mbs-journal.de

Figure 3. a) %Degradation and b) digital images of BDB-crosslinked PVA mats incubated at pHs ranging at 5–10.4 for 24 h as well as SEM images incubated at acidic c) pH = 5.4, d) physiological pH = 7.4, and alkali pHs e) 8.4 and f) 9.4.

used to treat skin infection was chosen as a model compound and loaded in BDB-crosslinked PVA nanofibrous mats. The e-spinning and BDB crosslinking protocol was repeated except the aqueous PVA solution contained 10 wt% LF. **Figure 4a** shows their SEM images with average diameter of 151.5 ± 29.0 nm (Figure S9, Supporting Information, for diameter histogram), which appeared to be slightly larger compared to the "bare" BDB-crosslinked nanofibers (133.9 ± 21.2 nm), which could be due to the presence of the LF during electrospinning.

The skin is the largest organ in the body, and its main function is to protect the body from the external environment. One of the key mechanisms by which the skin exerts its protective role is through its pH. Typically, healthy skin and healing wounds are slightly acidic (pH = 5–6) due to keratinocytes secreting fatty

acids and amino acid compounds into the skin. Within this pH range, alkaline-based chemicals are neutralized, opportunistic bacteria growth is inhibited, and skin microbiota is encouraged. Chronic wounds compromise the integrity and functionality of the skin, disrupting lipid synthesis and pH balance of the skin. Therefore, the pH of chronic wounds is generally alkaline (pH = 7–9), which promotes bacterial colonization.[26]

The LF-loaded PVA mats were examined for pH-responsive release of encapsulated LF using UV–vis spectroscopy. LF is soluble in water and has absorption bands from 200–350 nm. UV spectra were recorded at increasing concentrations at pH = 5.4 (acidic), 7.4 (neutral), and 8.4 (alkali) (Figure S10, Supporting Information). However, parts of the UV spectrum of LF overlaps with BDB in the region at 200–300 nm (Figure S11, Supporting
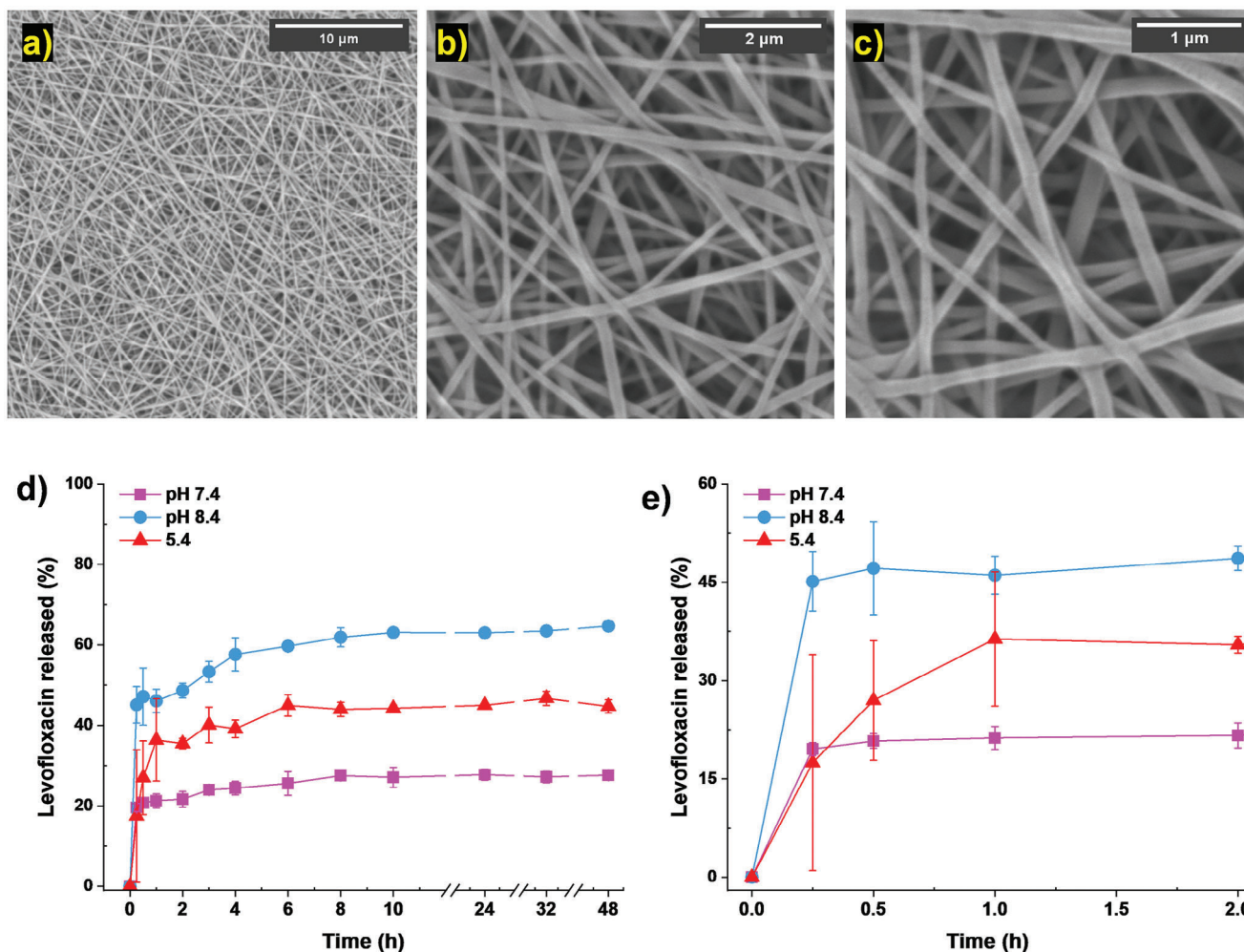
ADVANCED
SCIENCE NEWS
www.advancedsciencenews.com

[M]acro-molecular
Bioscience
www.mbs-journal.de

Figure 4. a–c) SEM images with different magnifications of LF-loaded BDB-crosslinked PVA nanofibers and %release of LF at pH = 5.4, 7.4, and 8.4 over incubation time in d) short and e) long time scale.

Information) and thus three LF calibration curves were constructed at 330 nm (Figure S12, Supporting Information), one for each pH due to LF's sensitivity to pH (Figure S13, Supporting Information). Next, pieces of LF-loaded BDB-crosslinked mats were immersed in aqueous buffer solution at pH = 5.4, 7.4, and 8.4 and the UV spectra of the aqueous solutions were recorded at given time intervals (Figure S14, Supporting Information). As seen in Figure 4b, %release rapidly increased within 30 min and slowly increased upon further incubation time for all three pHs. Interestingly, release reached 40% at acidic pH = 5.4% and 60% at pH = 8.4, while only 20% at pH = 7.4. The observed trend of %release versus pH is consistent with their acid-responsive degradation behavior (Figure 3).

LF-loaded BDB-crosslinked PVA mats were assessed for antimicrobial activity through a disk diffusion method to forecast their potential for wound dressings. Three bacterial species were examined, including the Gram-negative *Escherichia coli* (*E. Coli*; ATCC 25922) and *Salmonella enterica* Typhimurium (*S.* Typhimurium; ATCC 14028) and the Gram-positive *Staphylococcus aureus* (*S. aureus*; ATCC 29213). Our assay includes 10 ng ciprofloxacin (Cipro) as a positive control and LF-loaded non-

crosslinked PVA mat as a negative control. All tested groups were intended to receive the same amount of LF.

Figure 5 shows the results with their diameter of inhibition (DOI) and digital images as a measure of antimicrobial activity. Larger DOI values indicate greater antimicrobial activity. Promisingly, LF-loaded BDB-crosslinked mats had their DOI values nearly equal to the non-crosslinked samples for the two Gram-positive bacteria, and even slightly greater for the Gram-negative bacteria. These results confirm that the developed LF-loaded BDB-crosslinked PVA nanofibrous mats possess excellent antimicrobial activities against the Gram-positive and Gram-negative bacteria tested here. Note that the antimicrobial activity of the developed mats appeared to be greater against *E. coli* and *S. aureus*, compared with *S.* Typhimurium, which could be attributed to different susceptibilities of those bacteria to antibiotics. Furthermore, BDB-crosslinked mats had greater antimicrobial activity than mats crosslinked with GA (a conventionally used crosslinker for e-spun PVA nanofibers) (Figure S15, Supporting Information). As anticipated, the LF-loaded uncrosslinked PVA nanofibers mats displayed greater DOI against *E. coli* and *S. aureus* than did the LF-loaded BDB-crosslinked
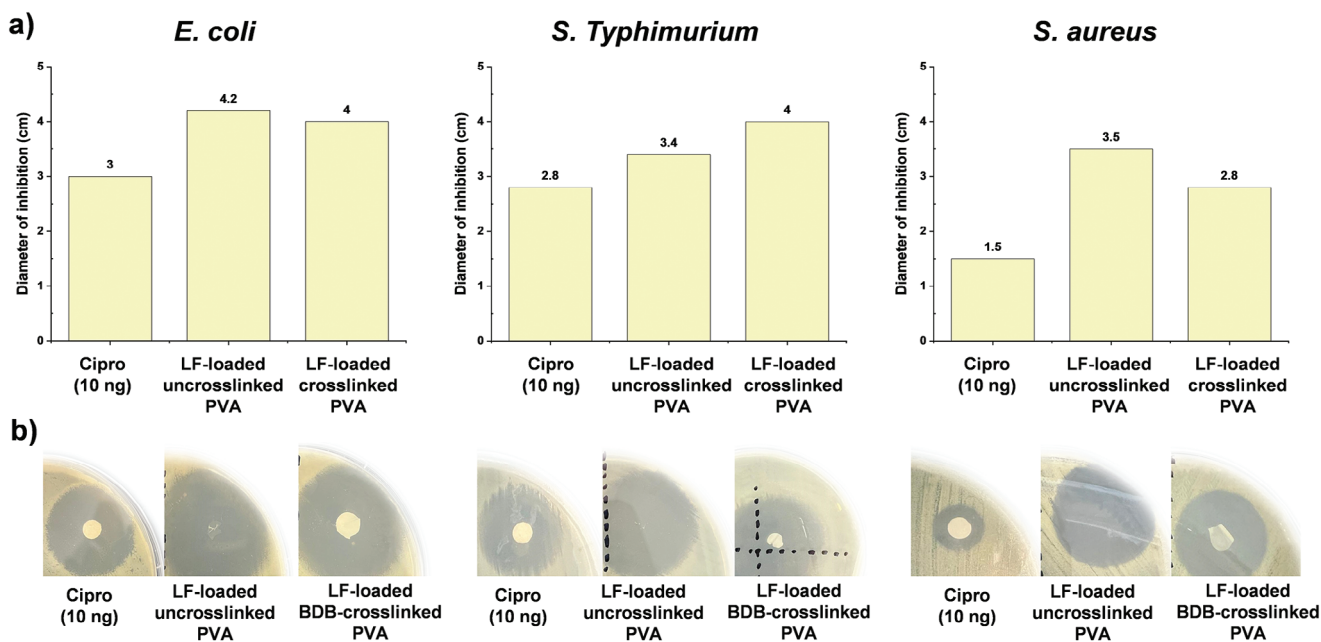
**ADVANCED
SCIENCE NEWS**

www.advancedsciencenews.com

[M] acro-molecular
Bioscience

www.mbs-journal.de

Figure 5. a) Diameter of inhibition (DOI) and b) digital images of three samples over Gram-negative *E. coli* and *S.* Typhimurium as well as Gram-positive *S. aureus*. Refer to Figure S16 (Supporting Information) for the entire petri dish caption.

mats. In an aqueous environment, uncrosslinked fibers did not exhibit the same stability as BDB-crosslinked fibers, prompting a faster PVA dissolution, a larger release of LF amount, and greater antibacterial effect. Beyond its well-known stabilizing role, BDB enabled control over drug release.

3. Conclusion

We explored a new approach to crosslinking e-spun PVA nanofibers. This approach used commercially available BDB to produce BE-PVA bonds that are largely degraded to their corresponding boronic acid and diol under elevated/reduced pH. By loading the nanofibers with a model drug during the crosslinking the pH-degradable PVA nanofibrous mats displayed controlled drug release. The intended goal is to use this methodology to develop wound dressings, but other applications are also possible. Qualitative analysis by FT-IR and quantitative analysis by gravimetry and gel content measurement confirmed the fabrication of dimensionally-stable PVA mats crosslinked through the formation of BE crosslinks. In addition, structure-property relation studies revealed that the incorporation of BDB (e.g., extent of crosslinking) appeared to be as low as 10% boronic acid to hydroxyl groups. Despite this, the gel contents of crosslinked mats were greater than 80% and the crosslinked mats retained their original fibrous forms during crosslinking procedure in organic solvents. The crosslinked fibers exhibit pH-responsive degradation and their degradation appeared to be greater in both acidic (pH = 5.4) and alkali (pH = 8.4) conditions through acid- or base-catalyzed hydrolysis of BE bonds, leading to rapid release kinetics of encapsulated LF in both alkali and acidic pHs. Promisingly, LF-loaded BE-crosslinked e-spun nanofibers exhibited excellent antimicrobial properties against both Gram-positive and Gram-

negative bacteria. These results demonstrate the proof of principle applicability of this approach toward the fabrication of BE-crosslinked PVA nanofibers for smart wound dressings exhibiting controlled/enhanced drug release.

4. Experimental Section

Instrumentation: Lab-made electrospinning setup included a spinneret directed toward a conventional stationary collector consisting of an aluminum foil target inside a Fisher model 630D incubator (Figure S1, Supporting Information, right). The collector was held at negative high voltage (e.g., −25 kV) while the needle/spinneret and metal-body incubator were grounded. A small muffin fan (75 mm, 6 W) was used in the incubator to circulate the air. The spinneret consisted of a square cut single-nozzle needle connected to a Spellman CZE1000R high-voltage direct current power supply (5–30 kV) and whose feeding rate was controlled by a syringe pump (LEGATO110 KD Scientific).

SEM images were obtained using a Phenom ProX with a resolution equivalent to, or less than, 8 nm and an acceleration voltage of 10 kV. Nanofibers were dried in vacuum oven for 24 h, mounted on a stub using double-face carbon tape, and coated with a 5 nm thick layer of gold using a Cressington 108 Auto Sputter Coater. Their average diameters were calculated from more than 100 nanofibers using ImageJ software. UV–vis spectra were recorded on a Cary 60 UV–vis Agilent Spectrophotometer using a rectangular quartz cuvette with an optical path length of 1 cm. FT-IR spectra were collected with a Thermo Scientific Nicolet iS5 spectrometer equipped with an iD5 attenuated total-reflection accessory. DSC measurements were performed in DSC Q20 Instrument with nitrogen flow (50 mL min^{-1}). For analysis, the samples were hermetically enclosed in an aluminum pan and equilibrated at −80 °C. Two cycles were run for each sample, each cycle consisting of heating up to 250 °C at a rate of 10 °C min^{-1} and subsequently cooling to −80 °C at a rate of 5 °C min^{-1}.

Materials: BDB (>95%), LF (>98%), phosphate buffered saline (PBS) tablets, Mueller Hinton Broth 2 (MHB) microbiology culture medium, agar powder (quality level 100), and PVA (89–98 kDa, 99+% hydrolyzed) were purchased from Millipore Sigma and used without any further purifi-

ADVANCED
SCIENCE NEWS

www.advancedsciencenews.com

Macromolecular
Bioscience
www.mbs-journal.de

cation unless otherwise mentioned. THF (ACS grade) was treated with 3 Å molecular sieves (8–12 mesh) to remove residual water.

Fabrication of E-Spun PVA Nanofibers: An aqueous solution of PVA (10% w/v) was prepared by dissolving PVA powder in deionized water at 80 °C under stirring for 60 min. Prior to electro-spinning, the formed solution was degassed and allowed to settle overnight. To fabricate well-defined PVA nanofibers, the solution (1 mL) was subsequently e-spun at a flow rate of 0.85 mL h^{-1} through a square cut BD 25G 1½ needle using the syringe pump with a nozzle-collector distance of 9 cm with an applied potential of 25 kV at 30 °C.

Crosslinking of E-Spun PVA Nanofibers with BDB: The fabricated PVA nanofibrous mats were immersed in THF with defined concentrations of BDB crosslinker as various mole equivalent ratios of BA/2OH of 0.25/1, 0.5/1, 1/1, and 2/1 for 48 h, yielding BDB-crosslinked PVA mats. They were dried in a vacuum oven set at 40 °C for 24 h and their masses were recorded. To estimate %insoluble PVA mats (or gel content), the mats were immersed in deionized water for 24 h and dried in vacuum oven set at 40 °C for 24 h.

pH-Responsive Degradation: Pieces of BDB-crosslinked e-spun nanofiber mats fabricated with the mole equivalent ratio of BA/2OH were immersed in 0.2 M buffer solutions at various pHs for 24 h. Acetate buffer for pH = 5.0–5.4, phosphate buffer for pH = 6.0–8.4, and carbonate buffer for pH = 9.4–10.4 were used. Either 1 M NaOH or 1 M HCl was used to adjust pH values.

Fabrication of LF-Loaded BDB-Crosslinked PVA Nanofibrous Mats: A 10% w/v PVA solution containing 10% w/w LF was prepared and subjected to electrospinning and crosslinking with BDB using the same protocols to fabricate fibrous mats with no LF.

pH-Responsive Drug Release Studies: Weighed pieces of LF-loaded BDB-crosslinked mat (≈15 mg) were immersed in 25 mL of either 0.2 M acetate buffer (pH = 5.4) or 0.2 M PBS solution (pH = 7.0 and 8.4) at 37 °C under stirring. Aliquots were taken periodically and their UV spectra were recorded. The experiments were performed under sink condition.

The calibration curve of LF was constructed with the absorbance at 330 nm over the concentration of LF at 1–15 µg mL^{-1}. Each solution was prepared by diluting a 20 µg mL^{-1} stock solution. The blank was the corresponding buffer solution, depending on which buffer solution was used for the release study or calibration curve.

Antimicrobial Studies: Kirby–Bauer disk diffusion method was employed in compliance with the European Committee on Antimicrobial Susceptibility Testing Guidelines. *E. Coli* (ATCC 25922), *S. aureus* (ATCC 29213), and *S. Typhimurium* (ATCC 14028) were seeded onto a petri dish with MHB culture medium (expected pH 7.3 ± 0.2 according to manufacturer) from an inoculum with a density of 0.5 McFarland Turbidity Standard (≈1–2 × 10^8 CFU mL^{-1}). The inoculum was prepared via direct colony suspension. Within 15 min of inoculation disk-shaped (8 mm diameter, 0.085 ± 0.05 mg), LF-loaded, BDB-crosslinked mats were placed on the surface of the inoculated agar and incubated at 35 ± 2 °C for 14 h. Cipro (10 ng) and LF-free BDB-crosslinked mats were examined as positive and negative control groups, respectively.

Supporting Information

Supporting Information is available from the Wiley Online Library or from the author.

Conflict of Interest

The authors declare no conflict of interest.

Data Availability Statement

The data that support the findings of this study are available in the supplementary material of this article.

[1] a) V. Falanga, R. R. Isseroff, A. M. Soulika, M. Romanelli, D. Margolis, S. Kapp, M. Granick, K. Harding, *Nat. Rev. Dis. Primers* **2022**, *8*, 50; b) M. Rodrigues, N. Kosaric, C. A. Bonham, G. C. Gurtner, *Physiol. Rev.* **2019**, *99*, 665; c) Y. Huang, L. Mu, X. Zhao, Y. Han, B. Guo, *ACS Nano* **2022**, *16*, 13022.

[2] S. Matoori, *ACS Appl. Bio. Mater.* **2023**, *6*, 2014.

[3] a) I. Negut, V. Grumezescu, A. M. Grumezescu, *Molecules* **2018**, *23*, 2392; b) T. Swanson, K. Ousey, E. Haesler, T. Bjarnsholt, K. Carville, P. Idensohn, L. Kalan, D. H. Keast, D. Larsen, S. Percival, *J. Wound. Care* **2022**, *31*, S10.

[4] K. Las Heras, M. Igartua, E. Santos-Vizcaino, R. M. Hernandez, *J. Controlled Release* **2020**, *328*, 532.

[5] A. E. Stoica, C. Chircov, A. M. Grumezescu, *Molecules* **2020**, *25*, 2699.

[6] a) H. Adelnia, R. Ensandoost, S. S. Moonshi, J. N. Gavgani, E. I. Vasafi, H. T. Ta, *Eur. Polym. J.* **2022**, *164*, 110974; b) B. Bolto, T. Tran, M. Hoang, Z. Xie, *Prog. Polym. Sci.* **2009**, *34*, 969; c) M. Wang, J. Bai, K. Shao, W. Tang, X. Zhao, D. Lin, S. Huang, C. Chen, Z. Ding, J. Ye, *Int. J. Polym. Sci.* **2021**, *2021*, 2225426; d) L. Shang, Y. Yu, Y. Liu, Z. Chen, T. Kong, Y. Zhao, *ACS Nano* **2019**, *13*, 2749.

[7] a) A. Zakrzewska, S. S. Zargarian, C. Rinoldi, A. Gradys, D. Jarząbek, M. Zanoni, C. Gualandi, M. Lanzi, F. Pierini, *ACS Mater Au.* **2023**, *3*, 464; b) M. Miraftab, A. N. Saifullah, A. Çay, *J. Mater. Sci.* **2014**, *50*, 1943.

[8] B. Golba, O. I. Kalaoglu-Altan, R. Sanyal, A. Sanyal, *ACS Appl. Polym. Mater.* **2021**, *4*, 1.

[9] a) J. H. Xie, Y. Lo, *J. Mater. Sci.* **2003**, *38*, 2125; b) J. Y. Wu, C. W. Ooi, C. P. Song, C. Y. Wang, B. L. Liu, G. Y. Lin, C. Y. Chiu, Y. K. Chang, *Carbohydr. Polym.* **2021**, *262*, 117910.

[10] a) D. Nataraj, R. Reddy, N. Reddy, *Eur. Polym. J.* **2020**, *124*, 109484; b) L. Gautam, S. G. Warkar, S. I. Ahmad, R. Kant, M. Jain, *Polym. Eng. Sci.* **2022**, *62*, 225.

[11] K. C. de Castro, E. K. Silva, M. G. N. Campos, L. H. I. Mei, *ACS Appl. Nano Mater.* **2022**, *5*, 12616.

[12] a) G. M. Scheutz, J. J. Lessard, M. B. Sims, B. S. Sumerlin, *J. Am. Chem. Soc.* **2019**, *141*, 16181; b) D. B. Tiz, F. A. Vicente, A. Kroflič, B. Likozar, *ACS Sustainable Chem. Eng.* **2023**, *11*, 13836.

[13] a) C. Huang, S. J. Soenen, J. Rejman, B. Lucas, K. Braeckmans, J. Demeester, S. C. De Smedt, *Chem. Soc. Rev.* **2011**, *40*, 2417; b) I. Altinbasak, S. Kocak, A. H. Colby, Y. Alp, R. Sanyal, M. W. Grinstaff, A. Sanyal, *Biomater. Sci.* **2023**, *11*, 813; c) M. Qi, X. Li, Y. Yang, S. Zhou, *Eur. J. Pharm. Biopharm.* **2008**, *70*, 445.

[14] a) K. Chen, Y. Li, Y. Li, Y. Tan, Y. Liu, W. Pan, G. Tan, *J. Nanobiotechnol.* **2023**, *21*, 237; b) M. Chen, Y. F. Li, F. Besenbacher, *Adv. Healthcare Mater.* **2014**, *3*, 1721.

**ADVANCED
SCIENCE NEWS**

www.advancedsciencenews.com

[M]acro-
molecular
Bioscience

www.mbs-journal.de

[15] a) A. G. Destaye, C. K. Lin, C. K. Lee, *ACS Appl. Mater. Interfaces* **2013**, *5*, 4745; b) H. Y. Huang, A. Skripka, L. Zaroubi, B. L. Findlay, F. Vetrone, C. Skinner, J. K. Oh, L. A. Cuccia, *ACS Appl. Bio. Mater.* **2020**, *3*, 7219; c) Y. Li, S. Yao, *Polym. Degrad. Stab.* **2017**, *137*, 229; d) G. Mugnaini, R. Gelli, L. Mori, M. Bonini, *ACS Appl. Polym. Mater.* **2023**, *5*, 9192.

[16] R. M. LoPachin, T. Gavin, *Chem. Res. Toxicol.* **2014**, *27*, 1081.

[17] a) A. M. Jazani, C. Shetty, H. Movasat, K. K. Bawa, J. K. Oh, *Macromol. Rapid. Commun.* **2021**, *42*, 2100262; b) Y. Hao, J. He, S. Li, J. Liu, M. Zhang, P. Ni, *J. Mater. Chem. B* **2014**, *2*, 4237; c) A. M. Jazani, N. Arezi, C. Shetty, J. K. Oh, *Mol. Pharmaceutics* **2021**, *19*, 1786.

[18] a) W. L. A. Brooks, B. S. Sumerlin, *Chem. Rev.* **2016**, *116*, 1375; b) S. Chatterjee, E. V. Anslyn, A. Bandyopadhyay, *Chem. Sci.* **2021**, *12*, 1585; c) S. Cho, S. Y. Hwang, D. X. Oh, J. Park, *J. Mater. Chem. A* **2021**, *9*, 14630; d) X. Zhang, Y. Zhao, S. Wang, X. Jing, *Mater. Chem. Front.* **2021**, *5*, 5534; e) A. Stubelius, S. Lee, A. Almutairi, *Acc. Chem. Res.* **2019**, *52*, 3108.

[19] a) Y. Guan, Y. Zhang, *Chem. Soc. Rev.* **2013**, *42*, 8106; b) G. T. Williams, A. C. Sedgwick, S. Sen, L. Gwynne, J. E. Gardiner, J. T. Brewster 2nd, J. R. Hiscock, T. D. James, A. T. A. Jenkins, J. L. Sessler, *Chem. Commun.* **2020**, *56*, 5516; c) A. Ali, S. Nouseen, S. Saroj, M. Shegane, P. Majumder, A. Puri, T. Rakshit, D. Manna, S. Pal, *J. Mater. Chem. B* **2022**, *10*, 7591; d) Y. Liang, M. Li, Y. Yang, L. Qiao, H. Xu, B. Guo, *ACS Nano* **2022**, *16*, 3194.

[20] a) M. Özcan, C. Kaya, F. Kaya, *Macromol. Mater. Eng.* **2023**, *308*, 2300150. b) Y. G. Jo, E. J. Shin, Y. J. Lee, W. S. Yoon, S. S. Han, Y. H. Lee, Y. R. Lee, S. K. Noh, Y. S. Gal, W. S. Lyoo, *J. Appl. Polym. Sci.* **2009**, *113*, 1733; c) A. F. Isik, N. O. S. Keskin, Y. Ulcay, *J. Text. Inst.* **2018**, *110*, 575.

[21] a) E. L. Daniels, J. R. Runge, M. Oshinowo, H. S. Leese, A. Buchard, *ACS Appl. Energy Mater.* **2023**, *6*, 2924; b) R. Nishiyabu, Y. Takahashi, T. Yabuki, S. Gommori, Y. Yamamoto, H. Kitagishi, Y. Kubo, *RSC Adv.* **2019**, *10*, 86.

[22] M. A. P. Nunes, P. M. P. Gois, M. E. Rosa, S. Martins, P. C. B. Fernandes, M. H. L. Ribeiro, *Tetrahedron* **2016**, *72*, 7293.

[23] M. Mukai, W. Ma, K. Ideta, A. Takahara, *Polymer* **2019**, *178*, 121581.

[24] L. Yao, T. W. Haas, A. Guiseppi-Elie, G. L. Bowlin, D. G. Simpson, G. E. Wnek, *Chem. Mater.* **2003**, *15*, 1860.

[25] D. G. Hall, *Chem. Soc. Rev.* **2019**, *48*, 3475.

[26] a) N. Tiwari, E. R. Osorio-Blanco, A. Sonzogni, D. Esporrin-Ubieto, H. Wang, M. Calderon, *Angew Chem. Int. Ed. Engl.* **2022**, *61*, e202107960; b) S. Hawkins, B. R. Dasgupta, K. P. Ananthapadmanabhan, *Int. J. Cosmet Sci.* **2021**, *43*, 474.